QED Weighting Function — Key Equations

The QED weighting function $\mathcal{G}$ is the pure-QED part of the master formula for the hadronic light-by-light (HLbL) contribution to the muon $g-2$, in the formulation of Refs. [1, 2].

Contents

1 Master formula

$$a_\mu^{\mathrm{HLbL}} = \frac{2m_\mu e^2}{3} \frac{1}{VT} \sum_{x_{\mathrm{op}}} \sum_{x,y,z} \frac{1}{2} \epsilon_{i,j,k} \left(x_{\mathrm{op}} - x_{\mathrm{ref}}(x,y,z) \right)_j \times (6e^4)\, \mathcal{H}_{k,\rho,\sigma,\lambda}(x_{\mathrm{op}},x,y,z)\, \mathcal{M}_{i,\rho,\sigma,\lambda}(x,y,z) \tag{1}$$

Two ingredients enter on the right-hand side:

- $\mathcal{H}$ — the hadronic four-point function, computed with lattice QCD.
- $\mathcal{M}$ — the QED weighting function (this note), computed analytically in infinite volume from free muon and photon propagators.

2 Hadronic four-point function $\mathcal{H}$

2.1 Definition

The hadronic four-point function is the QCD expectation value of four electromagnetic currents:

$$(6e^4)\,\mathcal{H}_{k,\rho,\sigma,\lambda}(x_{\mathrm{op}},x,y,z) = \langle T J_k(x_{\mathrm{op}}) J_\rho(x) J_\sigma(y) J_\lambda(z)\rangle_{\mathrm{QCD}} \tag{2}$$

$$J_\nu(x) = \sum_{q=u,d,s,c} e_q Z_V\, \bar{\psi}_q(x)\gamma_\nu\psi_q(x) \tag{3}$$

where Z_V is the lattice local vector current renormalization constant.

2.2 Diagram decomposition

After Wick contraction, $\mathcal{H}$ splits into diagram types:

$$\mathcal{H} = \mathcal{H}^{\mathrm{con}} + \mathcal{H}^{\mathrm{discon}} + \mathcal{H}^{\text{sub-leading-discon}} + \mathcal{H}^{\mathrm{charm}} \tag{4}$$

- $\mathcal{H}^{\mathrm{con}}$ — light and strange quark connected diagrams (nonzero in the $SU(3)$ flavor limit).
- $\mathcal{H}^{\mathrm{discon}}$ — light and strange quark disconnected diagrams; the quark loops must be connected by gluons to contribute.
- $\mathcal{H}^{\text{sub-leading-discon}}$ — sub-leading disconnected diagrams, which vanish in the $SU(3)$ flavor limit.
- $\mathcal{H}^{\mathrm{charm}}$ — all diagrams involving charm quark loops.

2.3 Wick-contracted forms (without permutations)

All other factors in the master formula (1) are symmetric under permutations of x, y, z, so only a subset of Wick contractions needs to be computed, with appropriate multiplicity factors.

Connected diagram.

$$\begin{aligned} 6e^4\,\mathcal{H}^{\text{con-no-perm}}_{\nu,\rho,\sigma,\kappa}(x_{\mathrm{op}},x,y,z) = -6\Big\langle \mathrm{Re}\sum_{q=u,d,s} e_q^4 \mathrm{Tr}\Big(&\gamma_\nu S_q(x_{\mathrm{op}},x)\gamma_\rho S_q(x,z) \\ &\times \gamma_\kappa S_q(z,y)\gamma_\sigma S_q(y,x_{\mathrm{op}})\Big)\Big\rangle_{\mathrm{QCD}} \end{aligned} \tag{5}$$

Disconnected diagram.

$$\begin{aligned} 6e^4\,\mathcal{H}^{\text{discon-no-perm}}_{\nu,\rho,\sigma,\kappa}(x_{\mathrm{op}},x,y,z) = 3\Big\langle &\sum_{q'=u,d,s} e_{q'}^2 \mathrm{Tr}\Big(\gamma_\nu S_{q'}(x_{\mathrm{op}},x)\gamma_\rho S_{q'}(x,x_{\mathrm{op}})\Big) \\ &\times \sum_{q=u,d,s} e_q^2 \mathrm{Tr}\Big(\gamma_\kappa S_q(z,y)\gamma_\sigma S_q(y,z) \\ &\quad - \big\langle \gamma_\kappa S_q(z,y)\gamma_\sigma S_q(y,z)\big\rangle_{\mathrm{QCD}}\Big)\Big\rangle_{\mathrm{QCD}} \end{aligned} \tag{6}$$

where S_q denotes the quark propagator. In practice these are evaluated with two point-source propagators.

2.4 Current conservation relation

Unlike the connected part, $\mathcal{H}^{\text{discon-no-perm}}$ by itself satisfies current conservation in the continuum and infinite-volume limit:

$$\sum_{x_{\text{op}}} \mathcal{H}^{\text{discon-no-perm}}_{k,\rho,\sigma,\lambda}(x_{\text{op}}, x, y, z) = 0 \tag{7}$$

This is what permits the alternative choice $x_{\text{ref-discon}} = x$ for the disconnected diagrams (see Eq. (14)).

3 Spin projection $\mathcal{M}$

The muon spin structure is extracted by projecting $\mathcal{G}$ onto the magnetic part:

$$\mathcal{M}_{i,\rho,\sigma,\lambda}(x, y, z) = \frac{1}{2} \operatorname{Tr}\left[\frac{1}{6}\, i^3\, \mathcal{G}_{\rho,\sigma,\lambda}(x, y, z)\, \Sigma_i\right], \qquad \Sigma_k = \frac{\epsilon_{i,j,k}\, \gamma_i \gamma_j}{2i} \tag{8}$$

- $1/2$ — from the spin projection operator $(1 + \gamma_t)/2$ in $\mathcal{G}$.
- $1/6$ — average over the permutations included in $\mathcal{G}$.

4 Construction of $\mathcal{G}$

Built in four steps:

$$\mathfrak{G} \xrightarrow{\text{Hermitian symmetrization}} \mathfrak{G}^{(1)} \xrightarrow{\text{subtraction}} \mathfrak{G}^{(2)} \xrightarrow{\text{6 permutations}} i^3\, \mathcal{G}$$

4.1 Step 1 — Muon-line function $\mathfrak{G}$

Free muon propagators S_μ and Feynman-gauge photon propagators G, with the muon source and sink taken to temporal infinity:

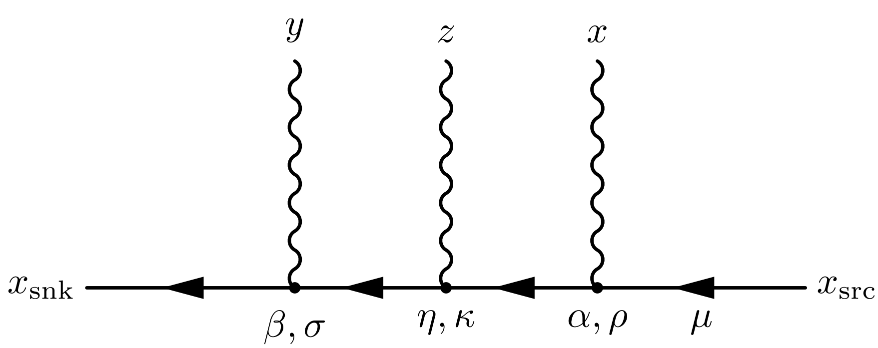

Figure 1: Muon-line function $\mathfrak{G}$: free muon propagators S_μ from x_{src} to x_{snk}, with photon propagators G from the vertices α, η, β to the hadronic-side points x, z, y (Eq. (9)).

$$\begin{aligned}\mathfrak{G}_{\sigma,\kappa,\rho}(y, z, x) = \lim_{t_{\text{src}}\to-\infty,\, t_{\text{snk}}\to\infty} e^{m_\mu(t_{\text{snk}} - t_{\text{src}})} \int_{\alpha,\beta,\eta,\vec{x}_{\text{snk}},\vec{x}_{\text{src}}} G(x, \alpha)\, G(y, \beta)\, G(z, \eta) \\ \times S_\mu(x_{\text{snk}}, \beta)\, i\gamma_\sigma\, S_\mu(\beta, \eta)\, i\gamma_\kappa\, S_\mu(\eta, \alpha)\, i\gamma_\rho\, S_\mu(\alpha, x_{\text{src}})\end{aligned} \tag{9}$$

This expression is infrared divergent; the divergence vanishes after projection to the magnetic part, or can be removed explicitly in Step 2.

4.2 Step 2 — Hermitian symmetrization $\mathfrak{G}^{(1)}$

Removes the infrared-divergent piece:

$$\mathfrak{G}^{(1)}_{\sigma,\kappa,\rho}(y,z,x) = \frac{1}{2}\,\mathfrak{G}_{\sigma,\kappa,\rho}(y,z,x) + \frac{1}{2}\left[\mathfrak{G}_{\rho,\kappa,\sigma}(x,z,y)\right]^{\dagger} \tag{10}$$

4.3 Step 3 — Subtraction $\mathfrak{G}^{(2)}$

Vector current conservation of the hadronic four-point function allows arbitrary subtractions without changing the final result:

$$\mathfrak{G}^{(2)}_{\sigma,\kappa,\rho}(y,z,x) = \mathfrak{G}^{(1)}_{\sigma,\kappa,\rho}(y,z,x) - \mathfrak{G}^{(1)}_{\sigma,\kappa,\rho}(z,z,x) - \mathfrak{G}^{(1)}_{\sigma,\kappa,\rho}(y,z,z) \tag{11}$$

Since $\mathfrak{G}^{(1)}(z,z,z) = 0$, this suppresses the weighting function where $|x-z|$ or $|y-z|$ is small — precisely where the lattice hadronic function has the largest discretization error — greatly reducing that error (key result of Ref. [1]).

4.4 Step 4 — Permutation sum

All six permutations of the three photon vertices $(x,\rho),(y,\sigma),(z,\kappa)$:

$$\begin{aligned} i^3\,\mathcal{G}_{\rho,\sigma,\kappa}(x,y,z) = {} & \mathfrak{G}^{(2)}_{\rho,\sigma,\kappa}(x,y,z) + \mathfrak{G}^{(2)}_{\sigma,\kappa,\rho}(y,z,x) + \mathfrak{G}^{(2)}_{\kappa,\rho,\sigma}(z,x,y) \\ & + \mathfrak{G}^{(2)}_{\kappa,\sigma,\rho}(z,y,x) + \mathfrak{G}^{(2)}_{\rho,\kappa,\sigma}(x,z,y) + \mathfrak{G}^{(2)}_{\sigma,\rho,\kappa}(y,x,z) \end{aligned} \tag{12}$$

5 Reference position x_{ref}

Connected diagrams. $x_{\text{ref}} = x_{\text{ref-far}}$ picks the vertex *not* adjacent to the shortest inter-vertex separation, or the centroid if there is no unique shortest separation:

$$x_{\text{ref-far}}(x,y,z) = \begin{cases} x & \text{if } |y-z| < \min(|x-y|,\ |x-z|) \\ y & \text{if } |x-z| < \min(|x-y|,\ |y-z|) \\ z & \text{if } |x-y| < \min(|x-z|,\ |y-z|) \\ \frac{1}{3}(x+y+z) & \text{otherwise} \end{cases} \tag{13}$$

Disconnected diagrams. Current conservation of $\mathcal{H}^{\text{discon-no-perm}}$ permits the simpler choice

$$x_{\text{ref-discon}} = x\,, \tag{14}$$

which decouples the x_{op} summation from y, z and agrees with $x_{\text{ref-far}}$ in the long-distance (π^0-exchange) region.

6 Notation

Symbol	Meaning
$\mathcal{G}$, $\mathcal{M}$	QED weighting function and its magnetic projection
$\mathfrak{G}$, $\mathfrak{G}^{(1)}$, $\mathfrak{G}^{(2)}$	Muon-line function: raw, symmetrized, subtracted
$\mathcal{H}$	Hadronic four-point function $\langle TJJJJ\rangle_{\mathrm{QCD}}$
J_ν	Electromagnetic current, Eq. (3)
e_q	Quark electric charge (in units of e)
Z_V	Lattice local vector current renormalization constant
S_μ, S_q	Muon and quark propagators
G	Feynman-gauge photon propagator
m_μ	Muon mass
V, T	Spatial volume and temporal extent of the lattice
x_{op}	Operator (external photon) insertion point
x, y, z	Internal photon vertices attached to the hadronic loop
x_{ref}	Reference position for the moment method

7 Comparison with the Mainz subtraction scheme

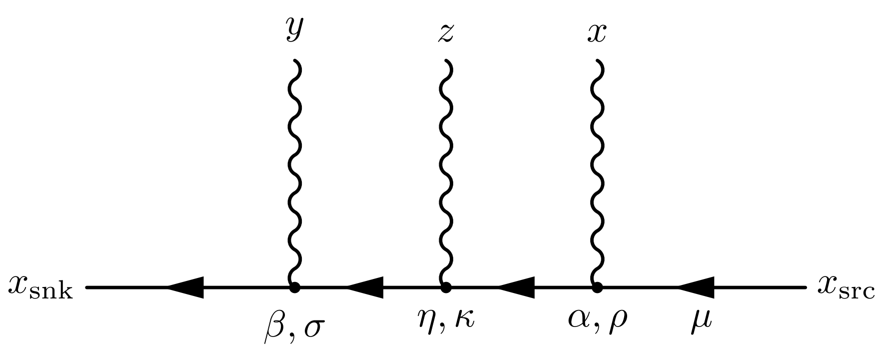

Figure 2: Muon-line function $\mathfrak{G}$ (repeated from Fig. 1): free muon propagators S_μ from x_{src} to x_{snk}, with photon propagators G from the vertices α, η, β to the hadronic-side points x, z, y.

The subtraction scheme used in this note (Step 3, Eq. (11)) removes the configurations $y = z$ and $x = z$:

$$\mathfrak{G}^{(2)}_{\sigma,\kappa,\rho}(y, z, x) = \mathfrak{G}^{(1)}_{\sigma,\kappa,\rho}(y, z, x) - \mathfrak{G}^{(1)}_{\sigma,\kappa,\rho}(z, z, x) - \mathfrak{G}^{(1)}_{\sigma,\kappa,\rho}(y, z, z) \tag{15}$$

Partial sums of the master-formula summand are performed in $R_{\max} = \max(|x-y|, |y-z|, |x-z|)$, for both connected and disconnected diagrams.

The Mainz group's choice [3, 4] (using RBC/UKQCD's notation):

$$\begin{aligned}\mathfrak{G}^{(\mathrm{Mainz})}_{\sigma,\kappa,\rho}(y, z, x) =& \mathfrak{G}^{(1)}_{\sigma,\kappa,\rho}(y, z, x) && (16)\\ & - \partial^y_\sigma((y-x)_\alpha e^{-\Lambda m_\mu^2 (y-x)^2/2})\mathfrak{G}^{(1)}_{\alpha,\kappa,\rho}(x, z, x) && (17)\\ & - \partial^z_\kappa((z-x)_\alpha e^{-\Lambda m_\mu^2 (z-x)^2/2})\mathfrak{G}^{(1)}_{\sigma,\alpha,\rho}(y, x, x) && (18)\end{aligned}$$

where $\Lambda = 0.4$.

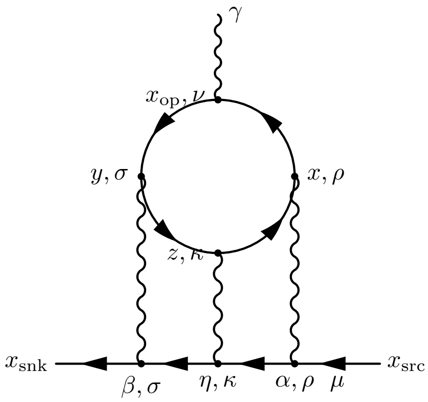

Figure 3: Connected diagram (Eq. (5)): a single quark loop with vertices x_{op}, ν (external photon), x, ρ, z, κ, and y, σ; internal photons connect x, z, y to the muon line.

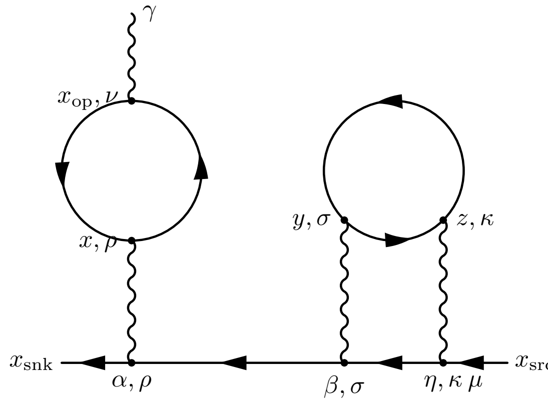

Figure 4: Disconnected diagram (Eq. (6)): two quark loops; one carries x_{op}, ν and x, ρ, the other z, κ and y, σ; internal photons connect the loops to the muon line.

In the Mainz scheme the partial sum is instead performed in "$|y|$" (in Mainz's notation), whose meaning depends on the diagram type (Figs. 3 and 4): for connected diagrams, "$|y|$" is the distance between the two vertices next to the external photon – $|x - y|$ in the figure; for disconnected diagrams, "$|y|$" is the distance between the two vertices on different quark loops – $|x - y|$ in the figure.

8 Code implementations

- **RBC weighting function** — implemented in Qlattice; example driver: `https://github.com/jinluchang/Qlattice/blob/master/examples-py-gpt/hlbl-muon-line.py`. (Documentation needs to be improved.)
- **Mainz QED kernel** — the KQED library: `https://github.com/RJHudspith/KQED`.

References

[1] Thomas Blum, Norman Christ, Masashi Hayakawa, Taku Izubuchi, Luchang Jin, Chulwoo Jung, and Christoph Lehner. Using infinite volume, continuum QED and lattice QCD for the hadronic light-by-light contribution to the muon anomalous magnetic moment. *Phys. Rev. D*, 96(3):034515, 2017. `arXiv:1705.01067`, `doi:10.1103/PhysRevD.96.034515`.

[2] Thomas Blum, Norman Christ, Masashi Hayakawa, Taku Izubuchi, Luchang Jin, Chulwoo Jung, Christoph Lehner, and Cheng Tu. Hadronic light-by-light contribution to the muon anomaly from lattice QCD with infinite volume QED at physical pion mass. *Phys. Rev. D*, 111(1):014501, 2025. `arXiv:2304.04423`, `doi:10.1103/PhysRevD.111.014501`.

[3] Nils Asmussen, En-Hung Chao, Antoine Gérardin, Jeremy R. Green, Renwick J. Hudspith, Harvey B. Meyer, and Andreas Nyffeler. Hadronic light-by-light scattering contribution to the muon g − 2 from lattice QCD: semi-analytical calculation of the QED kernel. *JHEP*, 04:040, 2023. `arXiv:2210.12263`, `doi:10.1007/JHEP04(2023)040`.

[4] En-Hung Chao, Renwick J. Hudspith, Antoine Gérardin, Jeremy R. Green, Harvey B. Meyer, and Konstantin Ottnad. Hadronic light-by-light contribution to $(g-2)_\mu$ from lattice QCD: a complete calculation. *Eur. Phys. J. C*, 81(7):651, 2021. `arXiv:2104.02632`, `doi:10.1140/epjc/s10052-021-09455-4`.